

Magnetic Resonance Tracking of Human CD34⁺ Progenitor Cells Separated by Means of Immunomagnetic Selection and Transplanted Into Injured Rat Brain

Pavla Jendelová,*†§ Vít Herynek,†‡ Lucia Urdziková,* Kateřina Glogarová,*† Šárka Rahmatová,** Ivan Fales,** Benita Andersson,* Pavel Procházka,¶ Josef Zamečník,# Tomáš Eckschlager,¶ Petr Kobylka,†** Milan Hájek,†‡ and Eva Syková*†§

*Institute of Experimental Medicine ASCR, Prague, Czech Republic

†Center for Cell Therapy and Tissue Repair, Charles University, Prague, Czech Republic

‡MR-Unit, Department of Diagnostic and Interventional Radiology, Institute for Clinical and Experimental Medicine, Prague, Czech Republic

§Department of Neuroscience, Charles University, Second Medical Faculty, Prague, Czech Republic

¶Department of Paediatric Haematology and Oncology and #Department of Pathology and Molecular Medicine, Charles University, Second Medical Faculty, Prague, Czech Republic

**Institute of Hematology and Blood Transfusion, Prague, Czech Republic

Magnetic resonance imaging (MRI) provides a noninvasive method for studying the fate of transplanted cells in vivo. We studied whether superparamagnetic nanoparticles (CD34 microbeads), used clinically for specific magnetic sorting, can be used as a magnetic cell label for in vivo cell visualization. Human cells from peripheral blood were selected by CliniMACS[®] CD34 Selection Technology (Miltenyi). Purified CD34⁺ cells were implanted into rats with a cortical photochemical lesion, contralaterally to the lesion. Twenty-four hours after grafting, the implanted cells were detected in the contralateral hemisphere as a hypointense spot on T₂ weighted images; the hypointensity of the implant decreased during the first week. At the lesion site we observed a hypointensive signal 10 days after grafting that persisted for the next 3 weeks, until the end of the experiment. Prussian blue and anti-human nuclei staining confirmed the presence of magnetically labeled human cells in the corpus callosum and in the lesion 4 weeks after grafting. CD34⁺ cells were also found in the subventricular zone (SVZ). Human DNA (a human-specific 850 base pair fragment of α -satellite DNA from human chromosome 17) was detected in brain tissue sections from the lesion using PCR, confirming the presence of human cells. Our results show that CD34 microbeads superparamagnetic nanoparticles can be used as a magnetic cell label for in vivo cell visualization. The fact that microbeads coated with different commercially available antibodies can bind to specific cell types opens extensive possibilities for cell tracking in vivo.

Key words: Cell transplantation; Magnetic resonance; Contrast agents; Hematopoietic stem cells; Photochemical lesion; Migration

INTRODUCTION

During the past two decades, dramatic progress in cellular transplantation and in vivo and ex vivo gene therapy has heightened optimism about future cures for injuries and diseases of the central nervous system (CNS). Some successful therapeutic approaches in animal models (rodents and primates) have already been transferred to the clinical area (11,13). The implantation of therapeutic cells in patients will require techniques that can noninvasively monitor their fate, behavior, and migra-

tion in the host organism. Methods have now been developed to incorporate sufficient amounts of superparamagnetic contrast agents into cells, enabling their detection in vivo using magnetic resonance (MR) imaging. Magnetically labeled cells are then visible on T₂ weighted images as a hypointensive signal. For the synthesis of the contrast agents, small crystals of magnetite Fe₃O₄ are predominantly used. The crystals are covered by a macromolecular shell, which can be chemically or biochemically modified (40,42,44,45). When specific antibodies are attached to the shell, the contrast agent can

Accepted February 3, 2005.

Address correspondence to Pavla Jendelová, Ph.D., Institute of Experimental Medicine ASCR, Vídeňská 1083, 142 20 Prague 4, Czech Republic. Tel: +420-224436781; Fax: + 420-224436799; E-mail: pavla.jendelova@lfmotol.cuni.cz

be specifically bound to tissue [for review see (4)]. Up to now, several types of contrast agents with a nanoparticle diameter in the range of 20 to 150 nm have been described, some of which are commercially available (40).

Bone marrow (BM) cells were reported recently to selectively target injured brain and spinal cord tissue and promote functional recovery (1,7,21,22,27,28). Some BM cells give rise to cells with a neural phenotype (22, 24). CD34⁺ cells—a subset of bone marrow cells—are known as hematopoietic progenitor cells (HPCs) (8). These cells, purified using a Miltenyi MACS sorter, are clinically used for hematopoiesis restoration (17,18,25). They are an important tool in clinical medicine, because they are an integral part of the BM transplant protocols used in leukemia therapy. In addition, HPCs can express neural genes (15) and may be a potential resource for generating neural stem cells in the injured CNS.

We studied if microbead superparamagnetic nanoparticles, normally used for specific magnetic sorting, can also be used as a magnetic cell label for in vivo cell visualization. Generally, HPCs can be separated from BM or granulocyte-colony stimulating factor (G-CSF) mobilized peripheral blood by means of immunomagnetic selection using anti-CD34 antibodies. For sorting, microbeads with a superparamagnetic iron-oxide core coated with a polysaccharide that is linked to an antibody are bound to the respective cell. The selected CD34⁺ cells retain the magnetic label attached to their surface, and because the size of the microbeads' superparamagnetic core is comparable to the size of the superparamagnetic core of MR contrast agents, microbeads may provide sufficient contrast on MR images. The labeled cells may therefore be visualized as a hypointense signal on T₂ weighted MR images.

MATERIALS AND METHODS

Cell Selection

CD34⁺ cells were prepared from human G-CSF mobilized peripheral blood progenitor cell concentrates using a CliniMACS (Miltenyi Biotech GmbH; Bergisch Gladbach, Germany) system and cryopreserved. The CD34⁺ cells were obtained from parental donors for patients who died before their planned haploidentical transplantation. The use of the cells for experimental purposes was based on the informed consent of the donors.

The first peripheral blood progenitor cell (PBPC) harvest was performed on the fifth day of daily G-CSF administration and the second harvest on the sixth day. The sorting of CD34⁺ cells was performed on the sixth day from the pooled PBPCs. The viability of the cells after cell selection was 99.3%, compared with the viability before selection, as measured by flow cytometry. The yield of the selection procedure was 40%.

For labeling of the CD34⁺ cells, the leukapheresis product was incubated with the CliniMACS CD34 Re-

agent. After washing away the excess unbound reagent, the automated selection was started. The CliniMACS system passed the antibody-labeled suspension through a column in which strong magnetic gradients were generated. The column retained the magnetically labeled CD34⁺ cells, while unwanted cells passed through and were collected in the negative fraction bag. The system performed several washing steps, disposing of most of the liquid into the buffer waste bag. The selected CD34⁺ cells were released from the column by removing the column from the magnetic field and eluting the cells into the cell collection bag. These highly purified cells were cryopreserved. The viability of cells after thawing was demonstrated indirectly by means of the cultivation of CFU-GM and CFU-mix using the MethoCult system (StemCell Technologies, Canada). Cryopreservation is routinely performed in our laboratory in the presence of dimethyl sulfoxide (DMSO, Sigma, St. Louis, MO) at a final concentration of 7.5% w/v, using an IceCube 1810 (Sy-Lab, Austria) programmable liquid nitrogen freezer.

Photochemical Lesion

We used a photochemical lesion as a model of thrombotic stroke (41). The lesion model uses a photochemical reaction in vivo to induce a thrombosis leading to a cerebral infarction. The method is virtually noninvasive because the skull is translucent for light at 560 nm, which is the wavelength used for inducing the photochemical reaction. As a result of the light exposure, Rose Bengal is excited and subsequently generates singlet molecular oxygen, thus it has the ability to induce photoperoxidative reactions. Damage to lipid membranes may provide the initial stimulus for platelet adhesion and subsequent aggregation, leading to thrombosis and infarction within 1 h (41). The formation of thrombotic plugs and adjacent red blood cell stasis within pial and parenchymal vessels is thus observed within the area exposed to the light.

Wistar male rats, 6–8 weeks old, were used throughout the study. Animals were divided into two groups: 1) rats with a cortical photochemical lesion and with contralaterally grafted CD34⁺ cells ($n = 8$), and 2) rats with a cortical photochemical lesion and with contralaterally injected phosphate-buffered saline (PBS) ($n = 4$).

The rats were anesthetized by isoflurane (2% isoflurane in air). Rose Bengal, a potent photosensitizing dye, was injected intravenously into the femoral vein (1 mg/100 g). A 1 × 2-mm area of the skull above the right cortex was exposed to the light from a halogen lamp for 10 min, while the rest of the skull was shielded with aluminum foil. The skin on the head was sutured, and the rats were left to recover and returned to their cages.

Grafting of CD34⁺ Progenitor Cells

Rats were anesthetized with isoflurane (Isofluran, Rhodia Organique Fine Limited, Bristol, UK) 7 days

after the photochemical lesion and mounted in a stereotactic frame. Using aseptic technique, a burr hole (1 mm) was made on the left side of the skull to expose the dura overlying the left cortex (22). Thawed CD34⁺ progenitor cells (7.5×10^6) were suspended in 5 μ l of PBS and slowly injected over a 10-min period using a Hamilton syringe into the contralateral hemisphere AP -1 mm, ML 2.5 mm, and DV 3.5 mm from bregma based on the atlas of Paxinos and Watson (30). The opening was closed by bone wax and the skin was sutured. For immunosuppression, cyclosporin (Novartis) 10 mg/kg IP was injected daily and Depo-Medrol[®] (Up-John) was administered weekly.

Magnetic Resonance Imaging

MR images of the brain were obtained using a 4.7 T Bruker spectrometer equipped with a homemade surface coil. The rats were anesthetized by passive inhalation of 1.5–2% isoflurane in air. Breathing was monitored during the measurements. Single sagittal, coronal, and transversal images were obtained by a fast gradient echo sequence for localizing the subsequent T₂ weighted transversal images measured by a standard turbo spin echo sequence. Sequence parameters were: repetition time $T_R = 2000$ ms, effective echo time $T_E = 42.5$ ms, turbo factor = 4, number of acquisitions AC = 16, field of view FOV = 3.5 cm, matrix 256 \times 256, slice thickness 0.5 mm, slice separation 1 mm. Two sets of interleaved transversal images were measured to cover the whole brain (22). All animals were scanned once 24 h after lesion induction, then 1, 3, 10, 17, and 28 days after cell grafting.

To check the sensitivity of the MRI technique, we performed *in vitro* experiments in gelatin. Cell suspensions were suspended in 1.7% gelatin at final concentrations of 97,000, 48,500, 24,250, 12,100, 6050, 3000, 1500, or 750 cells/ μ l. Samples, together with a gelatin-only control, were scanned using a 4.7 T Bruker spectrometer. Phantoms containing labeled cells were measured by a similar T₂ weighted sequence with a different geometry: field of view FOV = 6 cm, matrix 256 \times 256, slice thickness 1 mm. Only one slice was measured in the case of phantoms.

Histology and Immunohistochemistry

Rats were sacrificed 4 weeks after transplantation. The animals were deeply anaesthetized with chloral hydrate; their chest was opened and transcardially perfused with physiological saline followed by 4% paraformaldehyde in phosphate buffer (pH 7.4). Fixed brains were dissected and immersed in PBS with 30% sucrose. Frozen coronal sections (40 μ m) were cut through the whole brain.

Transplanted CD34⁺ cells were detected by staining for iron to produce ferric ferrocyanide (prussian blue),

by mouse monoclonal anti-human nuclei antibody diluted 1:40 (Chemicon, Temecula), and by a mouse monoclonal antibody directed against CD34 (clone QBEND10, Immunotech, Co.), diluted 1:100. As a secondary antibody goat anti-mouse IgG Alexa 594 (Molecular Probes) was used for the anti-human nuclei assay, and the CD34 antigen-antibody complexes were visualized using a biotin-streptavidin detection system (LSAB2 System, HRP, DakoCytomation,) with 3,3'-diaminobenzidine as a chromogen (Fluka Chemie, GmbH.). To visualize the possible colocalization of human nuclei and cell type-specific markers in the same cells, double staining was employed. Sections were incubated with cell type-specific antibodies directed against neuronal nuclear antigen (NeuN), dilution 1:100 (Chemicon), or against glial fibrillary acidic protein (GFAP) for identifying astrocytes, dilution 1:2500 (DAKO), as well as with anti human-nuclei as described above. As a secondary antibody, goat anti-mouse IgG Alexa 488 (Molecular Probes) was used. Host macrophages were detected by ED1 (mouse monoclonal anti-rat monocytes and macrophages FITC conjugate; Biosource international, Camarillo, CA), diluted 1:100.

To confirm that after cryopreservation microbeads remain attached to the cell surface, electron microscopy was performed. For electron microscopic examination, thawed CD34⁺ progenitor cells were fixed at 4°C in 2.5% buffered glutaraldehyde for 1 h, followed by 1% osmium tetroxide for 2 h. The cells were dehydrated in ascending concentrations of ethanol, immersed in propylene oxide, and embedded in Epon 812 resin (Agar Scientific Ltd, Standsted England). The samples were cut in ultrathin sections (~60 nm). These sections were contrasted with 4% uranyl acetate and Reynold's lead citrate and examined in a Philips Morgagni 268 transmission electron microscope.

Iron Content Quantitative Analysis

The amount of iron present in the cells was determined after mineralization by spectrophotometry. Samples (2 ml) containing 6×10^7 cells were mineralized after the addition of 5 ml HNO₃ and 1 ml H₂O₂ in an ETHOS 900 microwave mineralizer (Milestone ETHOS 900, Sydney, Australia). Deionized water was added to reach a total volume of 100 ml. The iron content was determined using a Spectroflame M120S (Spectro Inc., Littleton, MA) calibrated with a standard solution of As-tasol (Analytika Ltd., Prague, Czech Republic). The measurements were repeated four times, and the average value was determined.

DNA Polymerase Chain Reaction

Genomic DNA was extracted from rat brains using the Wizard Genomic DNA Purification Kit (Promega Corporation, USA) according to the manufacturer's in-

structions. The presence of human-specific DNA within the rat brains was confirmed by polymerase chain reaction amplification of a 850-bp fragment of the α -satellite region of human chromosome 17 using primers corresponding to the primer pair 17a1/17a2 as described by Becker et al. (3). For PCR, AmpliTaq-Gold polymerase (Applied Biosystems, Foster City, CA) was used. The PCR reaction mixture contained 200 μ M each of the respective nucleotides, 250 nM of each primer, 2 mM $MgCl_2$, and 250 ng of genomic DNA template as described by Becker et al. (3). Following an initial DNA denaturation at 95°C for 10 min, 40 cycles comprising 95°C denaturation, 56°C annealing, and 72°C extension for 1 min each were performed, followed by a final extension step at 72°C for 10 min. Amplified DNA fragments were electrophoresed through 1.75% agarose gels and subsequently visualized through ultraviolet light after staining with ethidium bromide. Genomic DNA samples from peripheral blood leukocytes of healthy volunteers, as positive controls, and PCR quality water, as a negative control, were processed in parallel. Leukocytes were isolated from whole blood by lysing erythrocytes using FACS lysing solution (BD, San Jose, CA) then washing two times with sterile PBS.

All animal experiments were carried out in accordance with the European Communities Council Directive of November 24, 1986 (86/609/EEC).

RESULTS

Labeling of CD34⁺ Progenitor Cells With Microbeads

The cells were selected from human peripheral blood progenitor cell concentrates by means of immunomagnetic selection using a CliniMACS system (Miltenyi). Unlike the nanoparticles of the contrast agent Endorem, which enter the cell and thus are present in the cell cytoplasm (22,23), the microbeads are bound to the cell surface via antigen-antibody interaction. Therefore, we first determined that after cryopreservation, the microbeads remain bound to the cell surface. Transmission electron microscopy confirmed the presence of several iron oxide nanoparticles attached to the cell surface. (Fig. 1A, B).

In Vitro MRI Detection of CD34⁺ Progenitor Cells

In vitro measurements of cell suspensions in gelatin showed a visibly hypointense signal on MRI with cell concentrations of 6050 cells/ μ l and higher (Fig. 2A). Image voxel volume [i.e., the sample volume that produces a signal of one image pixel (in a 1-mm slice with an in-plane resolution of $273 \times 273 \mu$ m)] was 0.075 μ l and therefore contained approximately 450 cells ($6050 \times 0.075 = 453.8$). This means that contrast changes were visible when the image voxel contained at least 450 cells. Spectrophotometry revealed that the mean iron

concentration in a 100-ml sample containing 7.28×10^7 cells was 0.2 μ g/ml, which corresponds to an average value of 0.275 pg of iron per cell. This value is lower by an order of magnitude than in the case of cell labeling using other contrast agents that enter the cell (17 pg of iron per cell in the case of labeling with the contrast agent Endorem) (22); nevertheless, it still provides sufficient MR contrast.

In Vivo MRI of Grafted Cells

MR Imaging. The cortical photochemical lesion was visible on MR images 24 h after light exposure as a hyperintensive area (Fig. 2B). The hyperintensity is caused by an acute edema. In control (nonimplanted) animals the lesion remained visible during the whole experimental period as an inhomogeneity in the tissue texture (Fig. 2C). In brains with a photochemical lesion and contralaterally injected cells, the cell implants were clearly visible 24 h after grafting as a hypointense area at the injection site (Fig. 2D). The hypointense signal of the injected cell implant is caused by the magnetic label bound to the cell surface, because the label behaves as a superparamagnetic MR contrast agent. The hypointensity of the implant decreased during the first week (Fig. 2E) but remained visible for the entire measurement period. Ten days after grafting we observed a weak hypointense signal in the lesion (Fig. 2F) that persisted for the next 3 weeks (i.e., until the end of our observation period) (Fig. 2G), thus suggesting the presence of magnetically labeled cells in the lesion.

Histology. Four weeks after grafting, histology showed that prussian blue-positive cells and cells stained for human nuclei had entered the lesion (Fig. 1C, E), confirming the presence of magnetically labeled human cells in the lesion. Many labeled cells were also detected in the corpus callosum, suggesting a migration route from the contralateral hemisphere towards the lesion. When we used a mouse monoclonal antibody directed against CD34, CD34⁺ cells were detected not only in the corpus callosum and in the lesion, but also in the SVZ (Fig. 1F).

Polymerase Chain Reaction. Brain tissue sections from the injection site, from the lesioned area, and from PBS-injected animals were tested using the polymerase chain reaction (PCR) to detect a human-specific 850 base pair fragment of α -satellite DNA from human chromosome 17. Human DNA was detected in the lesion of grafted animals. No human-specific DNA was detected in PBS-injected animals (Fig. 3).

DISCUSSION

It has been shown that magnetic resonance imaging techniques can be used to monitor the fate of trans-

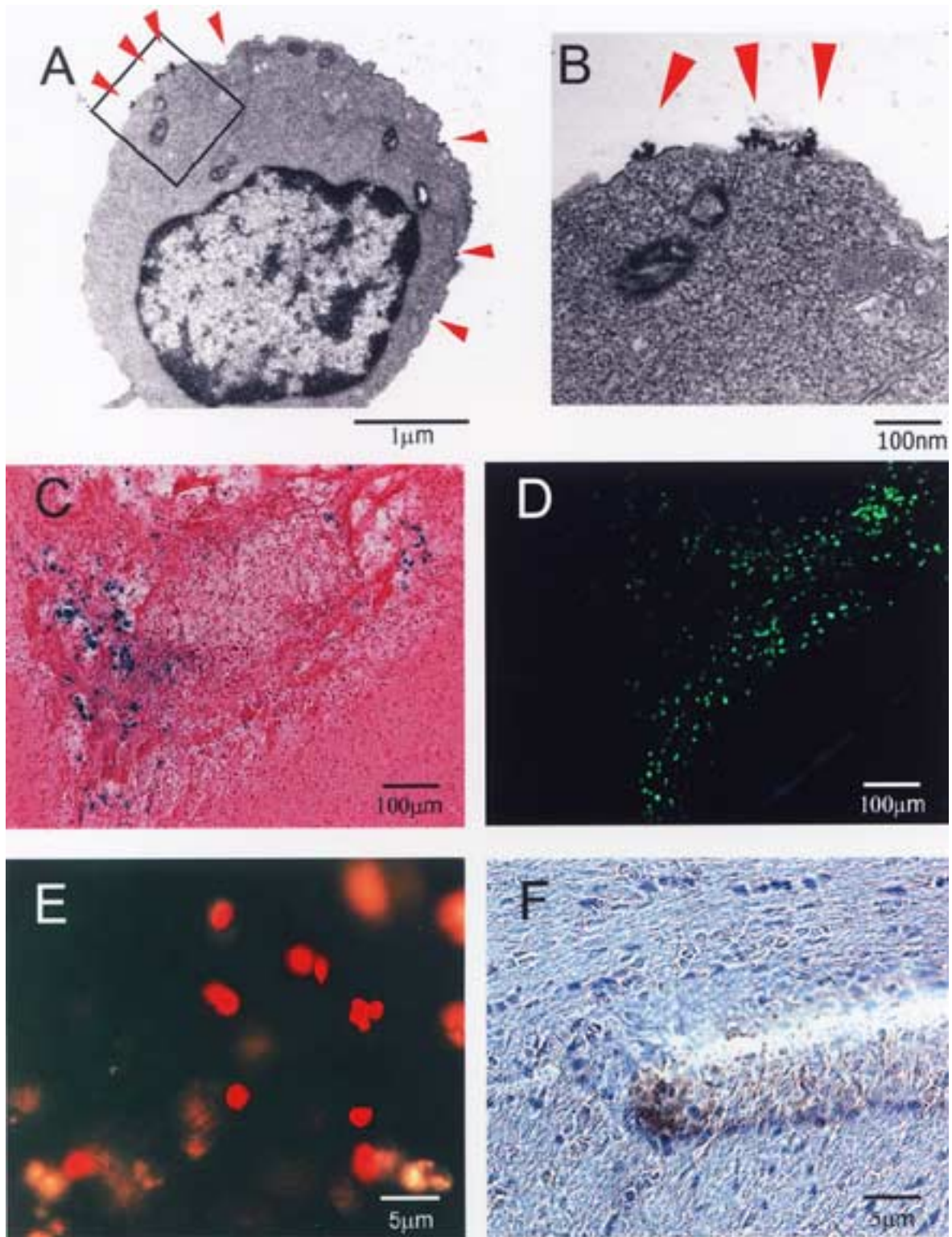


Figure 1. Labeling of CD34⁺ progenitor cells and their implantation into a rat brain with a photochemical lesion. (A) Transmission electron photomicrograph of a CD34⁺ cell showing the microbeads attached to the cell surface. Inset area shown at higher magnification in (B). (C) Histology performed 4 weeks postimplantation confirmed a large number of nanoparticle-labeled cells in the lesion (stained for prussian blue). (D) Serial section immunostained for ED1, showing that the presence of macrophages does not colocalize with staining for iron. (E) Human cells (positive staining for human nuclei) found in the lesion 4 weeks after grafting. (F) Staining with anti-CD34 revealed CD34⁺ cells in the subventricular zone.

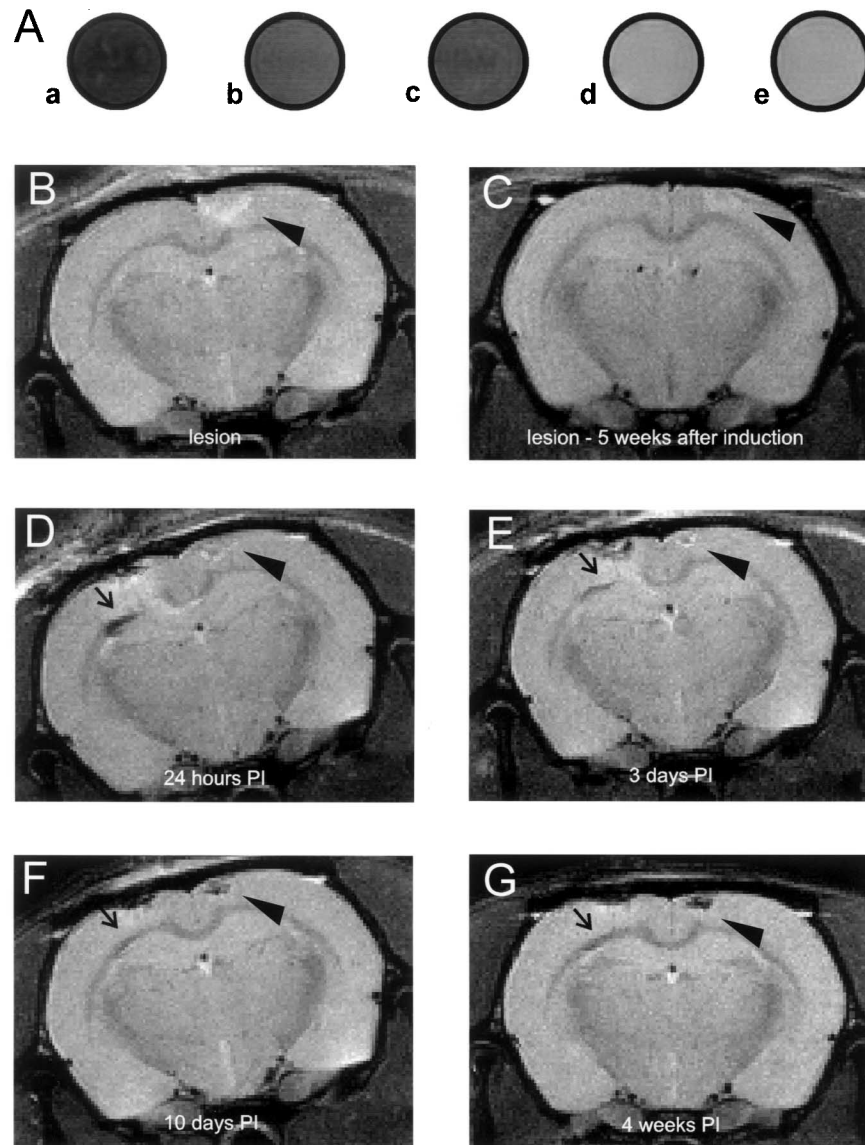


Figure 2. T₂ weighted images of phantoms, a cortical photochemical lesion, and implanted CD34⁺ cells. (A) MR images of a set of test tubes (phantoms) containing suspensions of microbead-labeled CD34⁺ cells in gelatin (sample a contains 97,000 cells/ μ l; b, 24,250; c, 6050; d, 3000; and e, 0 cells/ μ l). (B) A cortical photochemical lesion as a hyperintense area (arrowhead) on MR images 24 h after induction. (C) A cortical photochemical lesion in a control (nonimplanted) animal as an inhomogeneity in the tissue texture (arrowhead) on MR images 5 weeks after induction. (D) A cell implant (in the hemisphere contralateral to the lesion; arrow) as a hypointense area in MR images 24 h postinjection (PI). Note the hypointensity in the corpus callosum, while the lesion (arrowhead) remained hyperintense (E). A decreased signal (arrow) in the contralateral hemisphere 3 days after implantation. (F) A hypointense signal in the lesion (arrowhead) 10 days after grafting. (G) An enhanced signal in the lesion 4 weeks after grafting.

planted stem cells in a host organism. In our previous studies we monitored bone marrow stromal cells and mouse embryonic stem cells labeled with the contrast agent Endorem and grafted into rats with a brain or spinal cord injury (22,23). Similarly, several other groups

have reported that it is possible to visualize magnetically labeled cells in the brain or spinal cord after transplantation (4,6,12,20,26). However, all the magnetic labels (mainly different types of modified contrast agents) employed were intracellular. To enter the cell, different

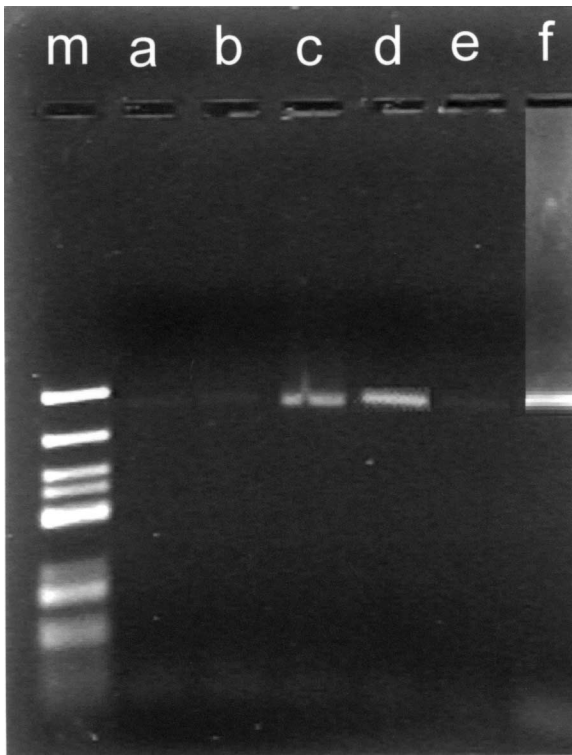


Figure 3. Polymerase chain reaction detection of a human-specific 850-bp fragment of α -satellite DNA on human chromosome 17 in brain sections 4 weeks after grafting. m: marker, a: negative control, b: lesion of PBS-injected animal, c: lesion of grafted animal, d: injection site of grafted animal, e: empty lane, f: positive control.

methods to facilitate entry are often required (e.g., lipofection, transfection agents, antibody–iron oxide particle constructs). Moreover, while commercially available contrast agents are clinically approved as blood pool agents, to be used as markers of implanted cells for clinical use in stem cell therapies further testing for cell toxicity and verification of CNS tolerance has to be done. In contrast, the microbeads used for immunomagnetic selection remain attached to the surface of a specific cell after sorting and have been safely transplanted into patients with hematological diseases (17,18). Bulte et al. (5) described experiments with human lymphocytes labeled with biotinylated antilymphocyte-directed monoclonal antibodies, to which streptavidin and subsequently biotinylated dextran-magnetite particles were coupled. Similar to our results, labeled lymphocyte suspensions enhanced negative contrast, though the experiments were done in a weaker magnetic field (2.0 Tesla). However, the study was done only *in vitro*, and the labeling kit used is not commercially available. In our study we confirmed that CD34 microbeads can be used as a magnetic label (a highly specific MR contrast

agent); they provide sufficient MR contrast although the average iron content per cell is an order of magnitude lower than in the case of cell labeling with Endorem and other contrast agents that enter the cell (22).

The data obtained from MR correlated with histological findings. PCR confirmed the presence of human cells in the lesion. To exclude that loose microbeads were taken up by macrophages, we performed ED1 staining for activated microglia/macrophages. Although we found strong ED1 positivity in the lesions, prussian blue staining did not colocalize with ED1 staining (Fig. 1C, D). In studies in which macrophage infiltration in different central nervous system disorders has been visualized with ultrasmall superparamagnetic iron oxide particles (USPIO) (9,10,32,34), the time course of loading macrophages with USPIO and their subsequent visualization on MR images did not correspond with the changes in MRI signal observed in our experiments. In rats (9,10,32,34), as well as in humans (31,38), a low intensity signal in the lesion due to infiltrating macrophages loaded with USPIO was already visible on T₂ weighted images at 24–72 h after the injection of USPIO into the blood stream, while in our experiments we observed a hypointensive signal in the lesion 10 days after grafting. Therefore, if the label were released *in vivo* and taken up by macrophages, the hypointensive signal would appear in the lesion during the first 72 h after cell injection and not 10 days after grafting. The macrophages observed in the lesion most likely infiltrated the lesion during the 7 days prior to cell grafting.

Bone marrow as an alternative source of adult stem cells may have practical advantages over embryonic stem cells and has been proposed for use as a source of autologous grafts. HPCs (characterized by the presence of the CD34 antigen) represent a major focus of current research (14,43). These cells have the capacity for extensive self-renewal and pluripotent differentiation and are used therapeutically to provide long-term bone marrow reconstitution in patients suffering from some leukemias, lymphomas, solid tumors, aplastic anemias, and metabolic disorders (19). Furthermore, human CD34⁺ cells have been shown to secrete numerous angiogenic factors, including VEGF, HGF, and IGF-1 (29). On the basis of these observations, clinical trials of cell transplantation in hindlimb (35,37) and cardiac ischemia (16) have been initiated with promising results. Human CD34⁺ cells can be collected from BM, cord blood, or from peripheral blood after cytokine mobilization. In our study we grafted human CD34⁺ progenitor cells, obtained from peripheral blood after G-CSF stimulation, into the lesioned rat brain. The human cells migrated from the injection site to the lesion and to the SVZ, where they survived throughout our observation period of 1 month. Our results are in agreement with the find-

ings of Asheuer (2), who reported the migration of human CD34⁺ cells into the brain after the intravenous injection of CD34⁺ cells into severe combined immunodeficient (SCID) mice. Furthermore, Goolsby et al. (15) described that human CD34⁺ cells, 6 months after implantation into adult mouse brain, expressed neuronal markers such as NeuN or CNPase and the glial marker GFAP. We did not observe any expression of NeuN or GFAP in our grafted cells 1 month after grafting. This may be due to our shorter observation time, because Goolsby et al. reported that the grafted cells remained CD34⁺ for the first 2 months. Similarly, Taguchi (36), who intravenously injected human CD34⁺ cells into mice with focal cerebral ischemia, did not observe any colocalization of transplanted CD34⁺ cells with NeuN or GFAP staining 2 weeks after grafting. Our finding that human CD34⁺ cells survived in the lesion and in the SVZ may support Taguchi's hypothesis (36) that CD34⁺ cells may play a positive role in neuroregeneration by inducing neovascularization in the ischemic zone, producing growth factors or cytokines and providing a favorable environment for neurogenesis.

Animal studies indicate that improved neural functioning can result from stem cell transplantation. Cell therapy has started to be used in patients suffering from brain and spinal cord injury, Parkinson's disease, or multiple sclerosis. The described immunolabeling of specific cell types with clinically approved microbeads may help to elucidate the fate of implanted stem cells and, in the future, to evaluate the effect of cell therapy in patients with various diseases of brain or spinal cord injury (33,39).

CONCLUSIONS

We conclude that microbead superparamagnetic nanoparticles, used for specific magnetic sorting, can also be used as a magnetic cell label for in vivo cell visualization with MRI. Microbead-labeled cells migrate and survive in the lesion. About 450 labeled cells are needed for MRI detection because the average iron content per cell is lower by an order of magnitude than in the case of intracellular contrast agents. However, the fact that microbeads coated with different commercially available antibodies can bind to specific cell types opens extensive experimental possibilities for cell tracking in vivo for immediate use in patients treated by stem cells.

ACKNOWLEDGMENTS: Support by grant numbers: LN 00A065, J13/98:11130004, AV0Z50390512, GAČR 304/03/1189.

REFERENCES

1. Akiyama, Y.; Radtke, C.; Honmou, O.; Kocsis, J. D. Remyelination of the spinal cord following intravenous delivery of bone marrow cells. *Glia* 39:229–236; 2002.
2. Asheuer, M.; Pflumio, F.; Benhamida, S.; Dubart-Kupper-schmitt, A.; Fouquet, F.; Imai, Y.; Aubourg, P.; Cartier, N. Human CD34⁺ cells differentiate into microglia and express recombinant therapeutic protein. *Proc. Natl. Acad. Sci. USA* 101:3557–3562; 2004.
3. Becker, M.; Nitsche, A.; Neumann, C.; Aumann, J.; Jung-hahn, I.; Fichtner, I. Sensitive PCR method for the detection and real-time quantification of human cells in xenotransplantation systems. *Br. J. Cancer* 87:1328–1335; 2002.
4. Bulte, J. W.; Duncan, I. D.; Frank, J. A. In vivo magnetic resonance tracking of magnetically labeled cells after transplantation. *J. Cereb. Blood Flow Metab.* 22:899–907; 2002.
5. Bulte, J. W.; Hoekstra, Y.; Kamman, R. L.; Magin, R. L.; Webb, A. G.; Briggs, R. W.; Go, K. G.; Hulstaert, C. E.; Miltenyi, S.; The, T. H.; et al. Specific MR imaging of human lymphocytes by monoclonal antibody-guided dextran-magnetite particles. *Magn. Reson. Med.* 25:148–157; 1992.
6. Bulte, J. W.; Zhang, S. C.; van Gelderen, P.; Herynek, V.; Jordan, E. K.; Duncan, I. D.; Frank, J. A. Neurotransplantation of magnetically labeled oligodendrocyte progenitors: Magnetic resonance tracking of cell migration and myelination. *Proc. Natl. Acad. Sci. USA* 96:15256–15261; 1999.
7. Chopp, M.; Li, Y. Treatment of neural injury with marrow stromal cells. *Lancet Neurol.* 1:92–100; 2002.
8. Civin, C. I.; Gore, S. D. Antigenic analysis of hematopoiesis: A review. *J. Hematother.* 2:137–144; 1993.
9. Dousset, V.; Ballarino, L.; Delalande, C.; Coussemaq, M.; Canioni, P.; Petry, K. G.; Caille, J. M. Comparison of ultrasmall particles of iron oxide (USPIO)-enhanced T2-weighted, conventional T2-weighted, and gadolinium-enhanced T1-weighted MR images in rats with experimental autoimmune encephalomyelitis. *Am. J. Neuroradiol.* 20:223–227; 1999.
10. Dousset, V.; Delalande, C.; Ballarino, L.; Quesson, B.; Seilhan, D.; Coussemaq, M.; Thiaudiere, E.; Brochet, B.; Canioni, P.; Caille, J. M. In vivo macrophage activity imaging in the central nervous system detected by magnetic resonance. *Magn. Reson. Med.* 41:329–333; 1999.
11. Dunnett, S. B.; Björklund, A.; Lindvall, O. Cell therapy in Parkinson's disease—stop or go? *Nat. Rev. Neurosci.* 2:365–369; 2001.
12. Franklin, R. J.; Blaschuk, K. L.; Bearchell, M. C.; Prestoz, L. L.; Setzu, A.; Brindle, K. M.; French-Constant, C. Magnetic resonance imaging of transplanted oligodendrocyte precursors in the rat brain. *Neuroreport* 10:3961–3965; 1999.
13. Freeman, T. B.; Olanow, C. W.; Hauser, R. A.; Nauert, G. M.; Smith, D. A.; Borlongan, C. V.; Sanberg, P. R.; Holt, D. A.; Kordower, J. H.; Vingerhoets, F. J. Bilateral fetal nigral transplantation into the postcommissural putamen in Parkinson's disease. *Ann. Neurol.* 38:379–388; 1995.
14. Fuchs, E.; Segre, J. A. Stem cells: A new lease on life. *Cell* 100:143–155; 2000.
15. Goolsby, J.; Marty, M. C.; Heletz, D.; Chiappelli, J.; Tashko, G.; Yarnell, D.; Fishman, P. S.; Dhib-Jalbut, S.; Bever, C. T., Jr.; Pessac, B.; Trisler, D. Hematopoietic progenitors express neural genes. *Proc. Natl. Acad. Sci. USA* 100:14926–14931; 2003.
16. Hamano, K.; Nishida, M.; Hirata, K.; Mikamo, A.; Li, T. S.; Harada, M.; Miura, T.; Matsuzaki, M.; Esato, K.

- Local implantation of autologous bone marrow cells for therapeutic angiogenesis in patients with ischemic heart disease: Clinical trial and preliminary results. *Jpn. Circ. J.* 65:845–847; 2001.
17. Handgretinger, R.; Klingebiel, T.; Lang, P.; Schumm, M.; Neu, S.; Geiselhart, A.; Bader, P.; Schlegel, P. G.; Greil, J.; Stachel, D.; Herzog, R. J.; Niethammer, D. Megadose transplantation of purified peripheral blood CD34(+) progenitor cells from HLA-mismatched parental donors in children. *Bone Marrow Transplant.* 27:777–783; 2001.
 18. Handgretinger, R.; Lang, P.; Ihm, K.; Schumm, M.; Geiselhart, A.; Koscielniak, E.; Hero, B.; Klingebiel, T.; Niethammer, D. Isolation and transplantation of highly purified autologous peripheral CD34(+) progenitor cells: Purging efficacy, hematopoietic reconstitution and long-term outcome in children with high-risk neuroblastoma. *Bone Marrow Transplant.* 29:731–736; 2002.
 19. Ho, A. Hematopoietic stem cell transplantation. New York: Marcel Dekker; 2000.
 20. Hoehn, M.; Kustermann, E.; Blunk, J.; Wiedermann, D.; Trapp, T.; Focking, M.; Arnold, H.; Hescheler, J.; Fleischmann, B. K.; Buhle, C. Monitoring of implanted stem cell migration in vivo: A highly resolved in vivo magnetic resonance imaging investigation of experimental stroke in rat. *Proc. Natl. Acad. Sci. USA* 100:1073–1078; 2002.
 21. Hofstetter, C. P.; Schwarz, E. J.; Hess, D.; Widenfalk, J.; El Manira, A.; Prockop, J. D.; Olson, L. Marrow stromal cells form guiding strands in the injured spinal cord and promote recovery. *Proc. Natl. Acad. Sci. USA* 96:2199–2204; 2002.
 22. Jendelová, P.; Herynek, V.; DeCroos, J.; Glogarová, K.; Andersson, B.; Hájek, M.; Syková, E. Imaging the fate of implanted bone marrow stromal cells labeled with superparamagnetic nanoparticles. *Magn. Reson. Med.* 50:767–776; 2003.
 23. Jendelová, P.; Herynek, V.; Urdzikova, L.; Glogarová, K.; Kroupová, J.; Bryja, V.; Andersson, B.; Burian, M.; Hájek, M.; Sykova, E. MR tracking of transplanted bone marrow and embryonic stem cells labeled by iron oxide nanoparticles in rat brain and spinal cord. *J. Neurosci. Res.* 76:232–243; 2004.
 24. Kopen, G. C.; Prockop, D. J.; Phinney, D. G. Marrow stromal cells migrate throughout forebrain and cerebellum, and they differentiate into astrocytes after injection into neonatal mouse brains. *Proc. Natl. Acad. Sci. USA* 96:10711–10716; 1999.
 25. Lang, P.; Handgretinger, R.; Niethammer, D.; Schlegel, P. G.; Schumm, M.; Greil, J.; Bader, P.; Engel, C.; Scheel-Walter, H.; Eyrich, M.; Klingebiel, T.; Ihm, K.; Geiselhart, A.; Koscielniak, E.; Hero, B.; Neu, S.; Stachel, D.; Herzog, R. J. Transplantation of highly purified CD34+ progenitor cells from unrelated donors in pediatric leukemia. *Blood* 101:1630–1636; 2003.
 26. Lee, I. H.; Bulte, J. W.; Schweinhardt, P.; Douglas, T.; Trifunovski, A.; Hofstetter, C.; Olson, L.; Spenger, C. In vivo magnetic resonance tracking of olfactory ensheathing glia grafted into the rat spinal cord. *Exp. Neurol.* 187: 509–516; 2004.
 27. Li, Y.; Chopp, M.; Chen, J.; Wang, L.; Gautam, S. C.; Xu, Y. X.; Zhang, Z. Intrastriatal transplantation of bone marrow nonhematopoietic cells improves functional recovery after stroke in adult mice. *J. Cereb. Blood Flow Metab.* 20:1311–1319; 2000.
 28. Lu, D.; Mahmood, A.; Wang, L.; Li, Y.; Lu, M.; Chopp, M. Adult bone marrow stromal cells administered intravenously to rats after traumatic brain injury migrate into brain and improve neurological outcome. *Neuroreport* 12: 559–563; 2001.
 29. Majka, M.; Janowska-Wieczorek, A.; Ratajczak, J.; Ehrenman, K.; Pietrkowski, Z.; Kowalska, M. A.; Gewirtz, A. M.; Emerson, S. G.; Ratajczak, M. Z. Numerous growth factors, cytokines, and chemokines are secreted by human CD34(+) cells, myeloblasts, erythroblasts, and megakaryoblasts and regulate normal hematopoiesis in an autocrine/paracrine manner. *Blood* 97:3075–3085; 2001.
 30. Paxinos, G.; Watson, C. The rat brain in stereotaxic coordinates. Sydney: Academic Press; 1986.
 31. Saleh, A.; Schroeter, M.; Jonkmanns, C.; Hartung, H. P.; Modder, U.; Jander, S. In vivo MRI of brain inflammation in human ischaemic stroke. *Brain* 127:1670–1677; 2004.
 32. Schroeter, M.; Saleh, A.; Wiedermann, D.; Hoehn, M.; Jander, S. Histochemical detection of ultrasmall superparamagnetic iron oxide (USPIO) contrast medium uptake in experimental brain ischemia. *Magn. Reson. Med.* 52: 403–406; 2004.
 33. Sivan-Loukianova, E.; Awad, O. A.; Stepanovic, V.; Bickenbach, J.; Schatteman, G. C. CD34+ blood cells accelerate vascularization and healing of diabetic mouse skin wounds. *J. Vasc. Res.* 40:368–377; 2003.
 34. Stoll, G.; Wesemeier, C.; Gold, R.; Solymosi, L.; Toyka, K. V.; Bendszus, M. In vivo monitoring of macrophage infiltration in experimental autoimmune neuritis by magnetic resonance imaging. *J. Neuroimmunol.* 149:142–146; 2004.
 35. Taguchi, A.; Ohtani, M.; Soma, T.; Watanabe, M.; Kinoshita, N. Therapeutic angiogenesis by autologous bone-marrow transplantation in a general hospital setting. *Eur. J. Vasc. Endovasc. Surg.* 25:276–278; 2003.
 36. Taguchi, A.; Soma, T.; Tanaka, H.; Kanda, T.; Nishimura, H.; Yoshikawa, H.; Tsukamoto, Y.; Iso, H.; Fujimori, Y.; Stern, D. M.; Naritomi, H.; Matsuyama, T. Administration of CD34+ cells after stroke enhances neurogenesis via angiogenesis in a mouse model. *J. Clin. Invest.* 114:330–3308; 2004.
 37. Tateishi-Yuyama, E.; Matsubara, H.; Murohara, T.; Ikeda, U.; Shintani, S.; Masaki, H.; Amano, K.; Kishimoto, Y.; Yoshimoto, K.; Akashi, H.; Shimada, K.; Iwasaka, T.; Imazumi, T. Therapeutic angiogenesis for patients with limb ischaemia by autologous transplantation of bone-marrow cells: A pilot study and a randomised controlled trial. *Lancet* 360:427–435; 2002.
 38. Trivedi, R. A.; JM, U-King-Im, J.-M.; Graves, M. J.; Cross, J. J.; Horsley, J.; Goddard, M. J.; Skepper, J. N.; Quartey, G.; Warburton, E.; Joubert, I.; Wang, L.; Kirkpatrick, P. J.; Brown, J.; Gillard, J. H. In vivo detection of macrophages in human carotid atheroma: Temporal dependence of ultrasmall superparamagnetic particles of iron oxide-enhanced MRI. *Stroke* 35:1631–1635; 2004.
 39. Valbonesi, M.; Giannini, G.; Migliori, F.; Dalla Costa, R.; Dejana, A. M. Cord blood (CB) stem cells for wound repair. Preliminary report of 2 cases. *Transfus. Apheresis Sci.* 30:153–156; 2004.
 40. Wang, Y. X.; Hussain, S. M.; Krestin, G. P. Superparamagnetic iron oxide contrast agents: Physicochemical characteristics and applications in MR imaging. *Eur. Radiol.* 11:2319–2331; 2001.
 41. Watson, B. D.; Dietrich, W. D.; Busto, R.; Wachtel, M. S.; Ginsberg, M. D. Induction of reproducible brain infarction by photochemically initiated thrombosis. *Ann. Neurol.* 17:497–504; 1985.

42. Weissleder, R.; Cheng, H. C.; Bogdanova, A.; Bogdanov, A., Jr. Magnetically labeled cells can be detected by MR imaging. *J. Magn. Reson. Imaging* 7:258–263; 1997.
43. Weissman, I. L. Translating stem and progenitor cell biology to the clinic: Barriers and opportunities. *Science* 287: 1442–1446; 2000.
44. Yeh, T.; Zhang, W.; Ildstad, S. T.; Ho, C. In vivo dynamic MRI tracking of rat T-cells labeled with superparamagnetic iron-oxide particles. *Magn. Reson. Med.* 33:200–208; 1995.
45. Yeh, T.; Zhang, W.; Ildstad, S. T.; Ho, C. Intracellular labeling of T-cells with superparamagnetic contrast agents. *Magn. Reson. Med.* 30:617–625; 1993.